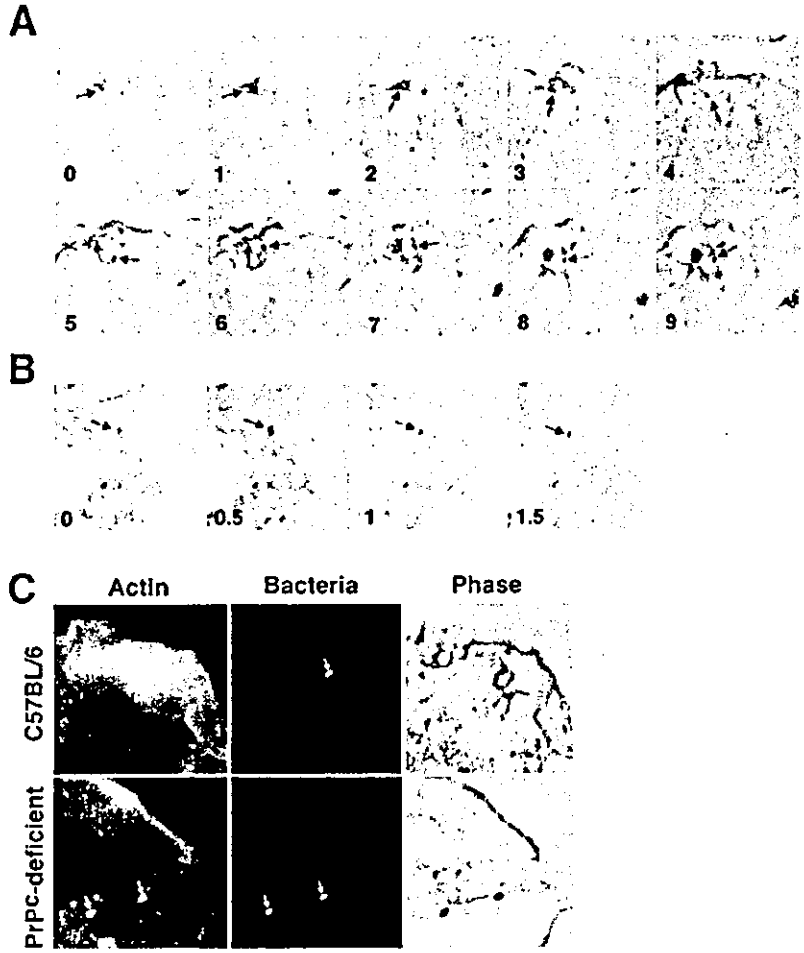

Figure 6. PrP^{C}-regulated swimming internalization of *B. abortus*. (A and B) Selected time lapse videomicroscopic images of wild-type *B. abortus* entry into macrophages from normal (A) or PrP^{c}-deficient C57BL/6 mice (B). Elapsed time in minutes is indicated at the bottom of each frame. Arrows point to bacteria. (C) Generalized actin polymerization after contact of macrophages with *B. abortus*. Bacteria were deposited onto macrophages from normal (top) or PrP^{c}-deficient mice (bottom) and then incubated for 5 min, fixed, and stained for actin filaments. Phase contrast microscopy of the corresponding microscopic fields are shown. Arrows point to bacteria.

be a similar mechanism to that of *B. abortus*. Effector proteins secreted by the type IV system of *B. abortus* have not been identified and this study is the first report describing a candidate effector-like protein secreted by the type IV system of *B. abortus*. Hsp60 are major antigens that elicit strong antibody responses in many bacteria (29). This includes bacteria that lack the type IV secretion system. Therefore, there is a possibility that Hsp60 might release by another secretion system and bind a denatured part of an effector protein of the type IV secretion system that might carry the Hsp60 to the bacterial surface.

It has been reported that PrP^{C} interacts with Hsp60 by using a *Saccharomyces cerevisiae* two-hybrid screening system (33). The PrP is the causative agent of neurodegenerative diseases such as Creutzfeld-Jakob disease in humans, bovine spongiform encephalopathy, and scrapie in sheep (34). The pathological, infectious form, PrP^{Sc}, is a β sheet aggregate, whereas the normal cellular isoform, PrP^{C}, consists of a largely α helical, autonomously folded COOH-terminal domain and an NH_2-terminal segment that is unstructured in solution (35). Conformational conversion of PrP^{C} into PrP^{Sc} has been suggested to involve a chaperone-like factor. GroEL of *E. coli* can catalyze the aggregation of chemically denatured and of folded, recombinant PrP in a model reaction in vitro (36). Based on a previous report, it was thought that surface-exposed Hsp60 of *B. abortus* could bind to PrP^{C} and catalyze the aggregation of PrP^{C} on macrophages. Consistent with this hypothesis, Hsp60 expressed on *L. lactis* could catalyze the aggregation of PrP^{C} on macrophages. However, PrP^{C} tail formation was not observed in macrophages infected with $Hsp60^{+}$ *L. lactis*. Hsp60 is not sufficient for PrP^{C} tail formation. In addition, swimming internalization and macropinosome formation were not observed in macrophages infected with $Hsp60^{+}$ *L. lactis*. PrP^{C} tail formation was required for bacterial swimming on macrophages and another bacterial factor, secreted by the type IV system, appears to be required for PrP^{C} tail formation.

B. abortus internalizes into macrophages by swimming on the cell surface for several minutes, with membrane sorting occurring during this period (6, 37). PrP^{C} tail formation is involved in the signaling pathway for swimming internalization because the PrP^{C} tail colocalized with Grb2 (unpublished data). Recently, evidence that PrP^{C} interacts

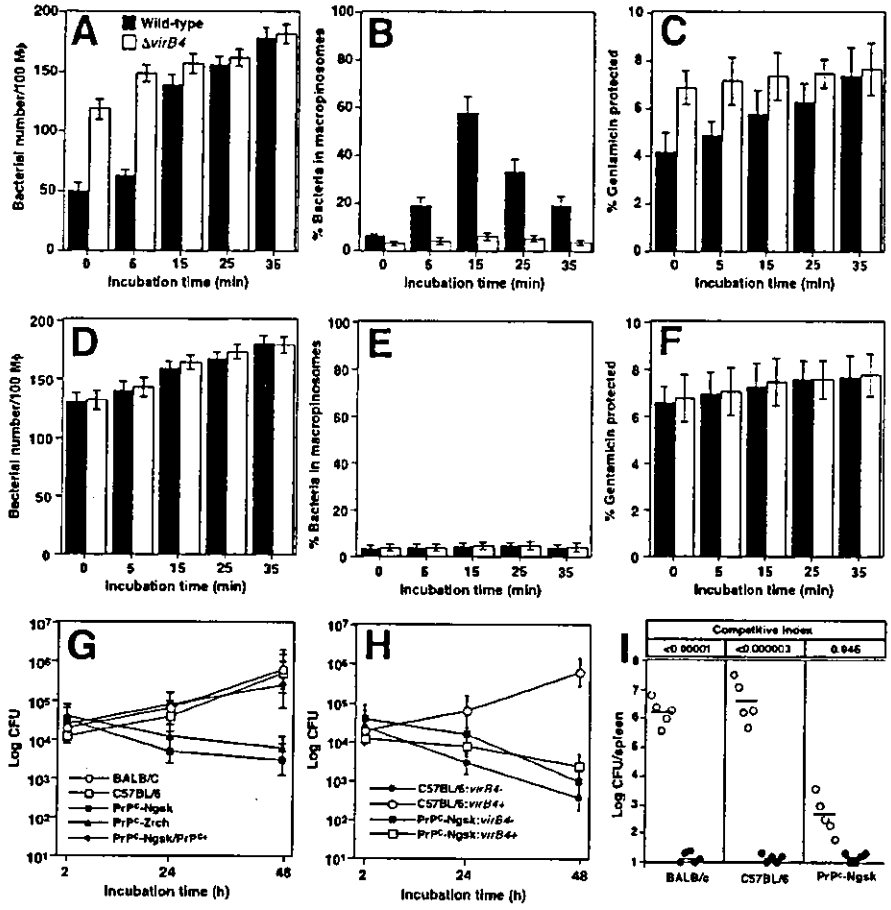

Figure 7. PrP^{C}-influenced *B. abortus* infection. (A–F) Wild-type (solid bars) or *virB4* mutant (open bars) were deposited onto macrophages from normal (A–C) or Ngsk PrP^{C}-deficient mice (D–F), and then incubated for the periods of time indicated. Uptake (A, C, D, and F) and macropinosome formation (B and E) were quantified as described in Materials and Methods. (A, B, D, and E) 100 macrophages were examined per coverslip. (C and F) Uptake efficiency by macrophages was determined by protection of internalized bacteria from gentamicin killing. Data are the average of triplicate samples from three identical experiments, and the error bars represent the standard deviation. (G and H) Intracellular replication of *B. abortus*. Macrophages from BALB/c, C57BL/6, Ngsk, or Zrch PrP^{C}-deficient mice, or PrP^{C} transgenic Ngsk PrP^{C}-deficient mice were infected with wild-type *B. abortus* (G), or *virB4* mutant (*virB4*−) and complemented strain (*virB4*+). (H). Data points and error bars represent the mean CFUs of triplicate samples from a typical experiment (performed at least four times) and their standard deviation, respectively. (I) Proliferation in mice. The CFUs of each strain were enumerated in the spleens of five mice from each group at 10 d after infection. For each mouse, the results are indicated by one open circle (log CFU of the wild-type) and one solid circle (log CFU of the *virB4* mutant). The means of the data are indicated by horizontal lines. The competitive index was calculated by dividing the mean ratio of mutant CFUs to the wild-type CFUs recovered from spleens by the ratio of the mutant CFUs to the wild-type CFUs in the inoculum.

with Grb2 was provided by the two-hybrid screening system (38). Grb2 is an adaptor protein involved in intracellular signaling from extracellular or transmembrane receptors to intracellular signaling molecules (39). The structure of Grb2 consists of a central SH2 domain flanked by two SH3 domains. The SH2 domain is responsible for interaction with tyrosine kinase, whereas the SH3 domains can bind to proline-rich motifs (40). Grb2 interacts through its SH3 domains with Wiskott-Aldrich syndrome protein (WASP), which plays a role in regulation of the actin cytoskeleton (41). WASP is a 64-kD protein expressed exclusively in hematopoietic cells (42). The carboxyl terminal portion of WASP contains regions that show homology to several actin-binding proteins, such as verprolin and cofilin, which may allow binding of WASP to filamentous actin (43). In regard to internalization of *B. abortus*, surface-exposed Hsp60 of *B. abortus* promotes aggregation of PrP^{C}, and PrP^{C} tail formation is induced by unidentified factor(s) secreted by the type IV system. The interaction of PrP^{C} tail with Grb2 will initiate cytoskeletal rearrangement and induce generalized membrane ruffling. Bacteria may obtain driving force for swimming internalization from membrane ruffling, like riding the wave of membrane until enclosed in macropinosomes. Consistent with this hypothesis, Grb2, which had interacted with PrP^{C} tail, was excluded in macropinosomes containing *B. abortus* (unpublished data). Presumably, the signal mediated by Grb2 is not required for replicative phagosome formation after macropinosome formation. Instead, a signal mediated by lipid rafts is needed for replicative phagosome formation (6).

The function of the *B. abortus virB* locus is essential for intracellular survival, both in cultured cells and in the mouse model (10, 11, 44–46). Our results of virulence for mice confirmed these previous works. The role of mouse macrophages in mediating resistance or susceptibility among mouse strains to some intracellular pathogens has been shown by studies of the *Ity/Lsh/Bcg* resistance model. Resistance to *Salmonella enterica* serovar Typhimurium, *Leishmania donovani*, and mycobacterial species is regulated by polymorphism of the *Nramp1* gene that controls macrophage function (47). Bovine Nramp1 is a major candidate for controlling the in vivo–resistant phenotype against *B. abortus* infection (48). Our previous study indicated that Niemann-Pick type C1 gene (NPC1) regulated the inter-

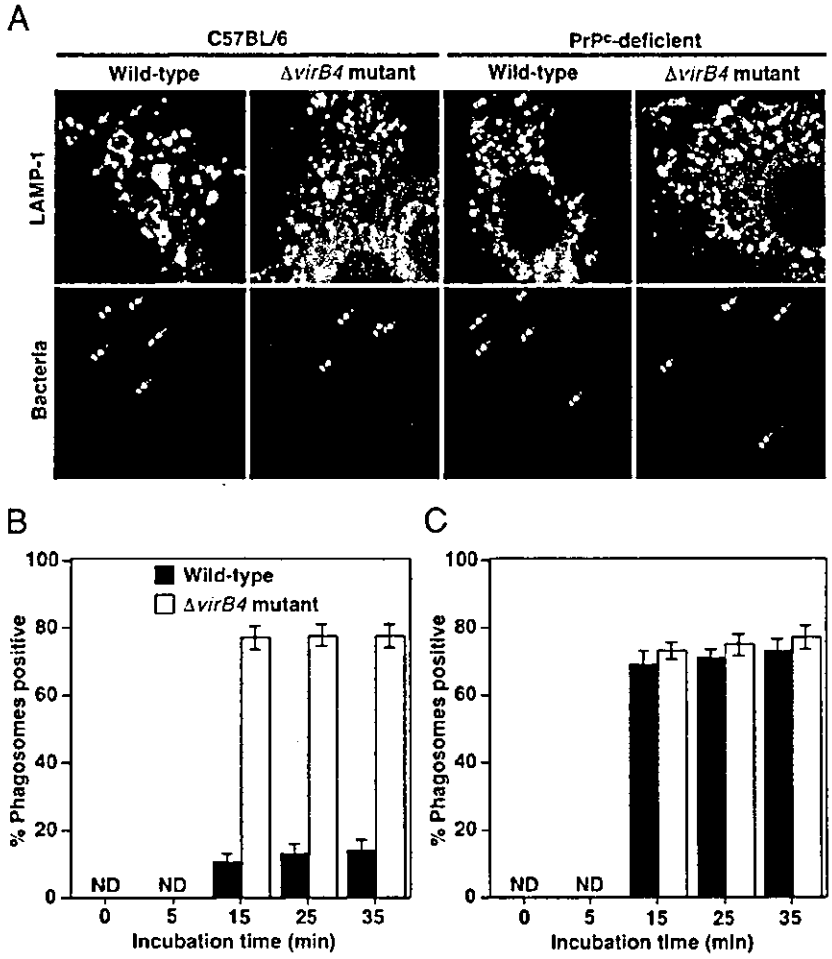

Figure 8. Colocalization of *B. abortus* with late endosomal and lysosomal marker LAMP-1 in macrophages from PrP^{C}-deficient mice, assessed by immunofluorescence microscopy. (A) Macrophages from C57BL/6 or PrP^{C}-deficient C57BL/6 mice were infected with wild-type or *virB4* mutant *B. abortus* for 35 min. (B and C) Wild-type (solid bars) or *virB4* mutant (open bars) were deposited onto macrophages from normal (B) or PrP^{C}-deficient mice (C), and then incubated for the periods of time indicated and probing with LAMP-1 was performed. % Phagosomes positive refers to percentage of internalized bacteria that showed costaining with LAMP-1, based on observation of 100 bacteria per coverslip. Data are the average of triplicate samples from three identical experiments, and error bars represent the standard deviation. ND, not detectable.

nalization and intracellular replication of *B. abortus* and also contributed to bacterial proliferation in mice (49). Macrophages from NPC1-deficient mice did not support internalization and intracellular replication of *B. abortus* (49). In this study, inhibition of internalization was not observed in macrophages from PrP^{C}-deficient mice. In NPC1-deficient mice macrophages, lipid raft-associated molecules, such as cholesterol, GM1 ganglioside, and GPI-anchored proteins, accumulated only in intracellular vesicles (49). In contrast, these molecules were present in both plasma membrane and intracellular vesicles of macrophages from PrP^{C}-deficient mice as well as macrophages from parent mice (unpublished data). Therefore, lipid raft-associated molecules on the plasma membrane are essential for the internalization of *B. abortus*, and PrP^{C} promotes the bacterial swimming internalization.

Lipid rafts are involved in infection by several intracellular pathogens. For example, macropinosomes containing *L. pneumophila* included lipid raft-associated molecules (50). GPI-anchored proteins were present in *Toxoplasma gondii* and *Plasmodium falciparum* vacuoles (51, 52). The intracellular parasite *L. donovani* can actively inhibit the acquisition of flotillin-1–enriched lipid rafts by phagosomes and the maturation of these organelles (53). Lipid platforms have been implicated in the budding of HIV and influenza virus (54, 55). The compartmentalization of Ebola and Marburg viral proteins within lipid rafts during viral assembly and budding has also been shown (56). In addition, PrP was attached to membranes by a GPI-anchor that associated with lipid rafts, and a recent study showed that conversion of raft-associated PrP^{C} to the protease-resistant state required insertion of PrP^{Sc} into contiguous membrane (57). Thus, lipid rafts, including PrP^{C}, may have an important role as a gateway for the intracellular trafficking of pathogens (58).

Current treatment of acute brucellosis requires combined regimen of antibiotics and is conditioned by the fact that brucellae are facultative intracellular pathogen. Thus, it is important to treat patients with drugs that penetrate macrophages. This fact seems to be responsible for the long duration of the disease and the high incidence of relapses. To this end, the study of the immunogenicities of antigens and their use in combination with new systems is very important for the development of better vaccines or antimicrobial agents. New strategies are also necessary to prevent brucel-

losis while avoiding the disadvantages of the currently used live vaccines for animals. The study of host–pathogen molecular interactions raises the possibility of novel vaccines or antimicrobial agents. The results of our study thus provide a potential new target for prevention of infection by intracellular pathogens.

We wish to thank Drs. Ben Adler and Hyeng-il Cheun for critical reading of the manuscript, Drs. Stanley B. Prusiner and Patrick Tremblay for PrP^{C}-deficient mice, and Drs. Chihiro Sasakawa and Toshihiko Suzuki for valuable discussion.

This work was supported, in part, by grants from The 21st Century Center of Excellence Program (A-1) and Scientific Research (12575029 and 13770129), Japan Society for the Promotion of Science.

Submitted: 15 November 2002
Revised: 23 April 2003
Accepted: 23 April 2003

References

1. Acha, P., and B. Szyfres. 1980. Zoonosis and Communicable Diseases Common to Man and Animals. Pan American Health Organization, Washington, DC. pp. 28–45.
2. Zavala, I., A. Nava, J. Guerra, and C. Quiros. 1994. Brucellosis. *Infect. Dis. Clin. North Am.* 8:225–241.
3. Baldwin, C.L., and A.J. Winter. 1994. Macrophages and *Brucella*. *Immunol. Ser.* 60:363–380.
4. Comerci, D.J., M.J. Martinez-Lorenzo, R. Sieira, J. Gorvel, and R.A. Ugalde. 2001. Essential role of the VirB machinery in the maturation of the *Brucella abortus*-containing vacuole. *Cell. Microbiol.* 3:159–168.
5. Pizarro-Cerda, J., E. Moreno, V. Sanguedolce, J.L. Mege, and J.P. Gorvel. 1998. Virulent *Brucella abortus* prevents lysosome fusion and is distributed within autophagosome-like compartments. *Infect. Immun.* 66:2387–2392.
6. Watarai, M., S.-I. Makino, Y. Fujii, K. Okamoto, and T. Shirahata. 2002. Modulation of *Brucella*-induced macropinocytosis by lipid rafts mediates intracellular replication. *Cell. Microbiol.* 4:341–356.
7. Naroeni, A., and F. Porte. 2002. Role of cholesterol and the ganglioside GM(1) in entry and short-term survival of *Brucella suis* in murine macrophages. *Infect. Immun.* 70:1640–1644.
8. Christie, P.J., and J.P. Vogel. 2000. Bacterial type IV secretion: conjugation systems adapted to deliver effector molecules to host cells. *Trends Microbiol.* 8:354–360.
9. Delrue, R.M., M. Martinez-Lorenzo, P. Lestrate, I. Danese, V. Bielarz, P. Mertens, X. De Bolle, A. Tibor, J.P. Gorvel, and J.J. Letesson. 2001. Identification of *Brucella* spp. genes involved in intracellular trafficking. *Cell. Microbiol.* 3:487–497.
10. Sieira, R., D.J. Comerci, D.O. Sanchez, and R.A. Ugalde. 2000. A homologue of an operon required in *Brucella abortus* for virulence and intracellular multiplication. *J. Bacteriol.* 182: 4849–4855.
11. O'Callaghan, D., C. Cazevieille, A. Allardet-Servent, M.L. Boschiroli, G. Bourg, V. Foulongne, P. Frutos, Y. Kulakov, and M. Ramuz. 1999. A homologue of the *Agrobacterium tumefaciens* VirB and *Bordetella pertussis* Ptl type IV secretion systems is essential for intracellular survival of *Brucella suis*. *Mol. Microbiol.* 33:1210–1220.
12. Horiuchi, M., N. Yamazaki, T. Ikeda, N. Ishiguro, and M. Shinagawa. 1995. A cellular form of prion protein (PrPC) exists in many non-neuronal tissues of sheep. *J. Gen. Virol.* 76:2583–2587.
13. Erdenebaatar, J., S. Sugar, A. Yondondorj, T. Nagabayashi, B. Shuto, M. Watarai, S.-I. Makino, and T. Shirahata. 2002. Serological analysis of *Brucella*-vaccinated and -infected domesticated animals by using the agar gel immunodiffusion test with *Brucella* polysaccharide in Mongolia. *J. Vet. Med. Sci.* 64: 839–841.
14. Watarai, M., S.-I. Makino, and T. Shirahata. 2002. An essential virulence protein of *Brucella abortus*, VirB4, requires an intact nucleoside triphosphate-binding domain. *Microbiology.* 148:1439–1446.
15. Kovach, M.E., P.H. Elzer, D.S. Hill, G.T. Robertson, M.A. Farris, R.M. Roop, II, and K.M. Peterson. 1995. Four new derivatives of the broad-host-range cloning vector pBBR1MCS, carrying different antibiotic-resistance cassettes. *Gene.* 166:175–176.
16. Sakuguchi, S., S. Katamine, N. Nishida, R. Moriuchi, K. Shigematsu, T. Sugimoto, A. Nakatani, Y. Kataoka, T. Houtani, S. Shirabe, et al. 1996. Loss of cerebellar Purkinje cells in aged mice homozygous for a disrupted PrP gene. *Nature.* 380:528–531.
17. Bueler, H., M. Fischer, Y. Lang, H. Bluethman, H.P. Lipp, S.J. DeArmond, S.B. Prusiner, M. Aguet, and C. Weissmann. 1992. Normal development and behaviour of mice lacking the neuronal cell-surface PrP protein. *Nature.* 356: 577–582.
18. Nishida, N., P. Tremblay, T. Sugimoto, K. Shigematsu, S. Shirabe, C. Petromilli, S.P. Erpel, R. Nakaoke, R. Atarashi, T. Houtani, et al. 1999. A mouse prion protein transgene rescues mice deficient for the prion protein gene from Purkinje cell degeneration and demyelination. *Lab. Invest.* 79:689–697.
19. Watarai, M., S. Funato, and C. Sasakawa. 1995. Interaction of Ipa proteins of *Shigella flexneri* with $\alpha5\beta1$ integrin promotes entry of the bacteria into mammalian cells. *J. Exp. Med.* 183:991–999.
20. Horiuchi, M., G.S. Baron, L.W. Xiong, and B. Caughey. 2001. Inhibition of interactions and interconversions of prion protein isoforms by peptide fragments from the C-terminal folded domain. *J. Biol. Chem.* 276:15489–15497.
21. Satoh, E., Y. Ito, Y. Sasaki, and T. Sasaki. 1997. Application of the extracellular alpha-amylase gene from *Streptococcus bovis* 148 to construction of a secretion vector for yogurt starter strains. *Appl. Environ. Microbiol.* 63:4593–4596.
22. Roop, R.M., II, M.L. Price, B.E. Dunn, S.M. Boyle, N. Sriranganathan, and G.G. Schurig. 1992. Molecular cloning and nucleotide sequence analysis of the gene encoding the immunoreactive *Brucella abortus* Hsp60 protein, BA60K. *Microb. Pathog.* 12:47–62.
23. Hemmingsen, S.M., C. Woolford, S.M. van der Vies, K. Tilly, D.T. Dennis, C.P. Georgopoulos, R.W. Hendrix, and R.J. Ellis. 1988. Homologous plant and bacterial proteins chaperone oligomeric protein assembly. *Nature.* 333:330–334.
24. Holo, H., and I.F. Nes. 1989. High-frequency transformation by electroporation of *Lactococcus lactis* subsp. *cremoris* grown with glycine in osmotically stabilized media. *Appl. Environ. Microbiol.* 57:333–340.
25. Watarai, M., H.L. Andrews, and R.R. Isberg. 2001. Formation of a fibrous structure on the surface of *Legionella pneumophila* associated with exposure of DotH and DotO proteins after intracellular growth. *Mol. Microbiol.* 39:313–329.

26. Abrami, L., M. Fivaz, P.E. Glauser, R.G. Parton, and F.G. van der Goot. 1998. A pore-forming toxin interacts with a GPI-anchored protein and causes vacuolation of the endoplasmic reticulum. *J. Cell Biol.* 140:525–540.
27. Moore, R.C., I.Y. Lee, G.L. Silverman, P.M. Harrison, R. Strome, C. Heinrich, A. Karunaratne, S.H. Pasternak, M.A. Chishti, Y. Liang, et al. 1999. Ataxia in prion protein (PrP)-deficient mice is associated with upregulation of the novel PrP-like protein doppel. *J. Mol. Biol.* 292:797–817.
28. Bukau, B., and A.L. Horwich. 1998. The Hsp70 and Hsp60 chaperone machines. *Cell.* 92:351–366.
29. Kaufmann, S.H. 1990. Heat shock proteins and the immune response. *Immunol. Today.* 11:129–136.
30. Craig, E.A., B.D. Gambill, and R.J. Nelson. 1993. Heat-shock proteins: molecular chaperones of protein biogenesis. *Microbiol. Rev.* 57:402–414.
31. Hoffman, P.S., and R.A. Garduno. 1999. Surface-associated heat shock proteins of *Legionella pneumophila* and *Helicobacter pylori*: roles in pathogenesis and immunity. *Infect. Dis. Obstet. Gynecol.* 7:58–63.
32. Garduno, R.A., E. Garduno, and P.S. Hoffman. 1998. Surface-associated Hsp60 chaperonin of *Legionella pneumophila* mediates invasion in a HeLa cell model. *Infect. Immun.* 66: 4602–4610.
33. Edenhofer, F., R. Rieger, M. Famulok, W. Wendler, S. Weiss, and E.-L. Winnacker. 1996. Prion protein PrP^C interacts with molecular chaperones of the Hsp60 family. *J. Virol.* 70:4724–4728.
34. Prusiner, S.B. 1998. Prions. *Proc. Natl. Acad. Sci. USA.* 95: 13363–13383.
35. Jackson, G.S., and A.R. Clarke. 2000. Mammalian prion proteins. *Curr. Opin. Struct. Biol.* 10:69–74.
36. Stockel, J., and F.U. Hartl. 2001. Chaperonin-mediated *de novo* generation of prion protein aggregates. *J. Mol. Biol.* 313: 861–872.
37. Kim, S., M. Watarai, S.-I. Makino, and T. Shirahata. 2002. Membrane sorting during swimming internalization of *Brucella* is required for phagosome trafficking decisions. *Microb. Pathog.* 33:225–237.
38. Spielhaupter, C., and H.M. Schatzl. 2001. PrP^S directly interacts with proteins involved in signaling pathways. *J. Biol. Chem.* 276:44604–44612.
39. Koch, C.A., D. Anderson, M.F. Moran, C. Ellis, and T. Pawson. 1991. SH2 and SH3 domains: elements that control interactions of cytoplasmic signaling proteins. *Science.* 252: 668–674.
40. Anderson, D., C.A. Koch, L. Grey, C. Ellis, M.F. Moran, and T. Pawson. 1990. Binding of SH2 domains of phospholipase C gamma 1, GAP, and Src to activated growth factor receptors. *Science.* 250:979–982.
41. She, H.Y., S. Rockow, J. Tang, R. Nishimura, E.Y. Skolnik, M. Chen, B. Margolis, and W. Li. 1997. Wiskott-Aldrich syndrome protein is associated with the adapter protein Grb2 and the epidermal growth factor receptor in living cells. *Mol. Biol. Cell.* 8:1709–1721.
42. Stewart, D.M., S. Treiber-Held, C.C. Kurman, F. Facchetti, L.D. Notarangelo, and D.L. Nelson. 1996. Studies of the expression of the Wiskott-Aldrich syndrome protein. *J. Clin. Invest.* 97:2627–2634.
43. Derry, J.M., H.D. Ochs, and U. Francke. 1994. Isolation of a novel gene mutated in Wiskott-Aldrich syndrome. *Cell.* 78: 635–644.
44. Foulongne, V., G. Boug, C. Cazavieille, S. Michaux-Charachon, and D. O'Callaghan. 2000. Identification of *Brucella suis* genes affecting intracellular survival in an in vitro human macrophage infection model by signature-tagged transposon mutagenesis. *Infect. Immun.* 68:1297–1303.
45. Hang, P.C., R.M. Tsolis, and T.A. Ficht. 2000. Identification of genes required for chronic persistence of *Brucella abortus* in mice. *Infect. Immun.* 68:4102–4107.
46. Sum, Y.-H., A.B. den Hartigh, R. de Lima Santos, L.G. Adams, and R.M. Tsolis. 2002. *virB*-mediated survival of *Brucella abortus* in mice and macrophages is independent of a functional inducible nitric oxide synthase or NADPH oxidase in macrophages. *Infect. Immun.* 70:4826–4832.
47. Forbes, J.R., and P. Gros. 2001. Divalent-metal transport by NRAMP proteins at the interface of host-pathogen interactions. *Trends Microbiol.* 9:397–403.
48. Barthel, R., J. Feng, J.A. Piedrahita, D.N. McMurray, J.W. Templeton, and L.G. Adams. 2001. Stable transfection of the bovine *NRAMP1* gene into murine RAW264.7 cells: effect on *Brucella abortus* survival. *Infect. Immun.* 69:3110–3119.
49. Watarai, M., S.-I. Makino, M. Michikawa, K. Yanagisawa, S. Murakami, and T. Shirahata. 2002. Macrophage plasma membrane cholesterol contributes to *Brucella abortus* infection of mice. *Infect. Immun.* 70:4818–4825.
50. Watarai, M., I. Derre, J. Kirby, J.D. Growney, W.F. Dietrich, and R.R. Isberg. 2001. *Legionella pneumophila* is internalized by a macropinocytotic uptake pathway controlled by the Dot/Icm system and the mouse *Lgn1* locus. *J. Exp. Med.* 194:1081–1095.
51. Mordue, D.G., N. Desai, M. Dustin, and L.D. Sibley. 1999. Invasion by *Toxoplasma gondii* establishes a moving junction that selectively excludes host cell plasma membrane proteins on the basis of their membrane anchoring. *J. Exp. Med.* 190: 1783–1792.
52. Lauer, S., J. VanWye, T. Harrison, H. McManus, B.U. Samuel, N.L. Hiller, N. Mohandas, and K. Haldar. 2000. Vacuolar uptake of host components, and a role for cholesterol and sphingomyelin in malarial infection. *EMBO J.* 19:3556–3564.
53. Dermine, J.-F., S. Duclos, J. Garin, F. St-Louis, S. Rea, R.G. Parton, and M. Desjardins. 2001. Flotillin-1-enriched lipid raft domains accumulate on maturing phagosomes. *J. Biol. Chem.* 276:18507–18512.
54. Scheiffele, P., A. Rietveld, T. Wilk, and K. Simons. 1999. Influenza viruses select ordered lipid domains during budding from the plasma membrane. *J. Biol. Chem.* 274:2038–2044.
55. Nguyen, D.H., and J.E. Hildreth. 2000. Evidence for budding of human immunodeficiency virus type 1 selectively from glycolipid-enriched membrane lipid rafts. *J. Virol.* 74: 3264–3272.
56. Bavari, S., C.M. Bosio, E. Wiegand, G. Ruthel, A.B. Will, T.W. Geisbert, M. Hevey, C. Schmaljohn, A. Schmaljohn, and M.J. Aman. 2002. Lipid raft microdomains: a gateway for compartmentalized trafficking of Ebola and Marburg viruses. *J. Exp. Med.* 195:593–602.
57. Baron, G.S., K. Wehrly, D.W. Dorward, B. Chesebro, and B. Caughey. 2002. Conversion of raft associated prion protein to the protease-resistant state requires insertion of PrP-res (PrP(Sc)) into contiguous membranes. *EMBO J.* 21:1031–1040.
58. Duncan, M.J., J.-S. Shin, and S.N. Abraham. 2002. Microbial entry through caveolae: variations on a theme. *Cell. Microbiol.* 4:783–791.

Vet Pathol 40:723–727 (2003)

Experimental Transmission of Abnormal Prion Protein (PrPsc) in the Small Intestinal Epithelial Cells of Neonatal Mice

M. Okamoto, H. Furuoka, M. Horiuchi, T. Noguchi, K. Hagiwara, Y. Muramatsu, K. Tomonaga, M. Tsuji, C. Ishihara, K. Ikuta, and H. Taniyama

Abstract. Using an immunohistochemical method, we attempted to detect the transmission of abnormal prion protein (PrPsc) to the enterocytes of the small intestine of neonatal mice by oral exposure with sheep brain affected by scrapie. Five 1-day-old neonatal mice were exposed by oral inoculation to the homogenized brain of a scrapie-affected sheep. In the small intestine of all mice 1 hour after inoculation, immunoreactivity with antinormal prion protein (PrPc) antibody was seen in the cytoplasm of villus enterocytes. This finding suggests transmission of abnormal PrPsc into the cytoplasm of enterocytes. In control mice treated with normal sheep brain, no PrPc signal was seen in enterocytes of the small intestine. Immunopositivity for neurofilament protein and glial fibrillary acidic protein was seen in the cytoplasm of enterocytes of mice inoculated with scrapie and normal sheep brain. This suggests that the enterocytes of neonatal mice can absorb PrPsc and other macromolecular proteins of the sheep brain affected by scrapie and may be more important than previously thought as a pathway for PrPsc transmission in neonatal animals.

Key words: Mice; PrPsc; absorption; enterocyte; immunohistochemistry.

Animal-transmissible spongiform encephalopathies or prion diseases, including ovine scrapie and bovine spongiform encephalopathy (BSE), are caused by acquisition of abnormal prion protein (PrPsc). Replication of the PrPsc depends critically on the host normal prion protein (PrPc), which develops into an abnormal, detergent-insoluble, proteinase-resistant isoform, PrPsc, in affected tissues such as the central nervous system (CNS) and lymphoid tissues.[3] However, how and when animals acquire PrPsc in the course of natural scrapie infection is not known. In experimental studies involving intragastric or oral inoculation of rodents with PrPsc from scrapie brain, PrPsc was detected in Payer's patches, gut-associated lymphoid tissues,[7,9,10] and ganglia of the enteric nervous systems before its detection in the CNS.[2,14] After the ingestion of PrPsc, uptake by the small intestine may follow either M-cell dependent or M-cell independent routes.[5] However, little is known about the transport mechanisms by which PrPsc reaches the germinal centers of lymphoid tissues from the gut lumen.

In neonatal animals, histologically, distended vacuoles

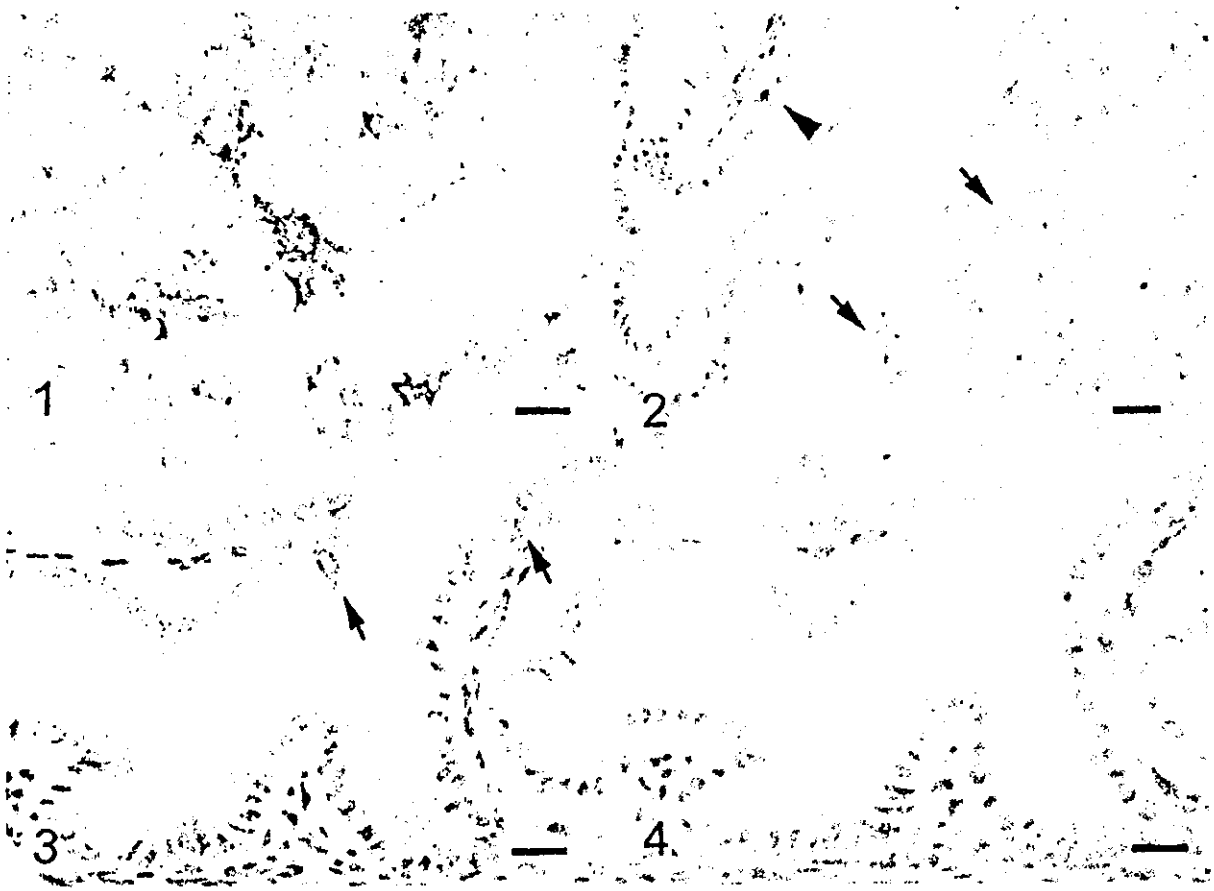

Fig. 1. Medulla oblongata: scrapie infected sheep, positive PrPc signal is seen in neuropil with spongiform change. ABC method, Mayer's hematoxylin counterstain. Bar = 20 mm.

Fig. 2. Small intestine; mouse, 1 hour after inoculation with homogenized sheep brain with scrapie. Positive signal for PrPc is present in the intralumeral sheep brain tissue (*arrows*) and in an enterocyte (*arrowhead*). ABC method. Mayer's hematoxylin counterstain. Bar = 30 mm.

Fig. 3. Small intestine; mouse, 1 hour after inoculation with homogenized sheep brain with scrapie. Positive signal for PrPc is present in the apical and basilar cytoplasm of villus enterocytes (*arrows*). ABC method, Mayer's hematoxylin counterstain. Bar = 20 mm.

Fig. 4. Small intestine: mouse, 1 hour after inoculation with homogenized sheep brain with scrapie. Immunostain omitting PrPc antibody shows no PrPc signal in enterocytes. ABC method, Mayer's hematoxylin counterstain. Bar = 20 mm.

containing colostral protein are frequently found in the cytoplasm of enterocytes lining villi of the small intestine, suggesting intestinal macromolecular uptake by pinocytosis during the first weeks after birth.[1,15] In this study, using immunohistochemical methods, we attempted to detect the entry of PrPsc into the enterocytes of the small intestine of neonatal mice following oral exposure to sheep brain containing abnormal prion of scrapie.

The first occurrence of ovine scrapie in Japan was reported in 1984.[13] Mice inoculated with fresh brain homogenates of an affected sheep showed the clinical signs and histopathologic lesions of scrapie after a long incubation period.[11]

Five 1-day-old neonatal mice were exposed by oral inoculation to sheep brain containing PrPsc. The sheep brain used for this study had been fixed in 10% formalin solution for 7 days and embedded in paraffin for 20 yrs.[13] Deparaffinized tissues (100 mg) of the medulla oblongata of the sheep were homogenized in 1 ml phosphate-buffered saline (PBS) with a polytron for 3 minutes, and 20 ml of homogenized brain was used for each peroral inoculation. For immunohistochemical controls, tissue sections were stained by procedures that omitted only the primary antibody. For negative controls, three neonatal mice were exposed by oral inoculation to normal sheep brain fixed in 10% formalin, embedded in paraffin, and extracted by identical procedures. All inoculated mice were sacrificed under anesthesia 1 hour after inoculation. Duodenum and jejunum were fixed in 4% paraformaldehyde in PBS for 24 hours and embedded in paraffin. Thin paraffin sections (4 mm) of the small intestine of mice

Fig. 5. Small intestine; mouse, 1 hour after inoculation with homogenized sheep brain with scrapie. There is PrPc signal mainly in the basilar cytoplasm of enterocytes at tip of the villus adjacent to the nucleus (arrows). ABC method, Mayer's hematoxylin counterstain. Bar = 10 mm.

and the medulla oblongata of the sheep brain affected by scrapie were deparaffinized and stained with hematoxylin and eosin (HE).

Histologic sections of sheep brain and mouse small intestine were stained immunohistochemically by the avidin-biotin-peroxidase complex (ABC) procedure (ABC-peroxidase staining kit (Elite: Vector Laboratories, Burlingame, CA). The specific antibody used in the present study was an affinity-purified polyclonal rabbit anti-PrPc antibody described in previous reports.[6,12] The synthetic peptide used as immunogen was B-103, corresponding to bovine PrP codons 103–121. This polyclonal antibody reacted strongly with PrPc-enriched fractions of brain tissues of cattle, sheep, and mouse on Western blots.[6]

Deparaffinized tissue sections for PrP immunostaining were autoclaved at 121 C for 30 minutes after immersion in 98% formic acid for 30 minutes and in 60 μg/ml proteinase K (Wako Pure Chemical Industries, Tokyo, Japan) in 0.1 mol/liter phosphate buffer saline for 5 minutes. Sections

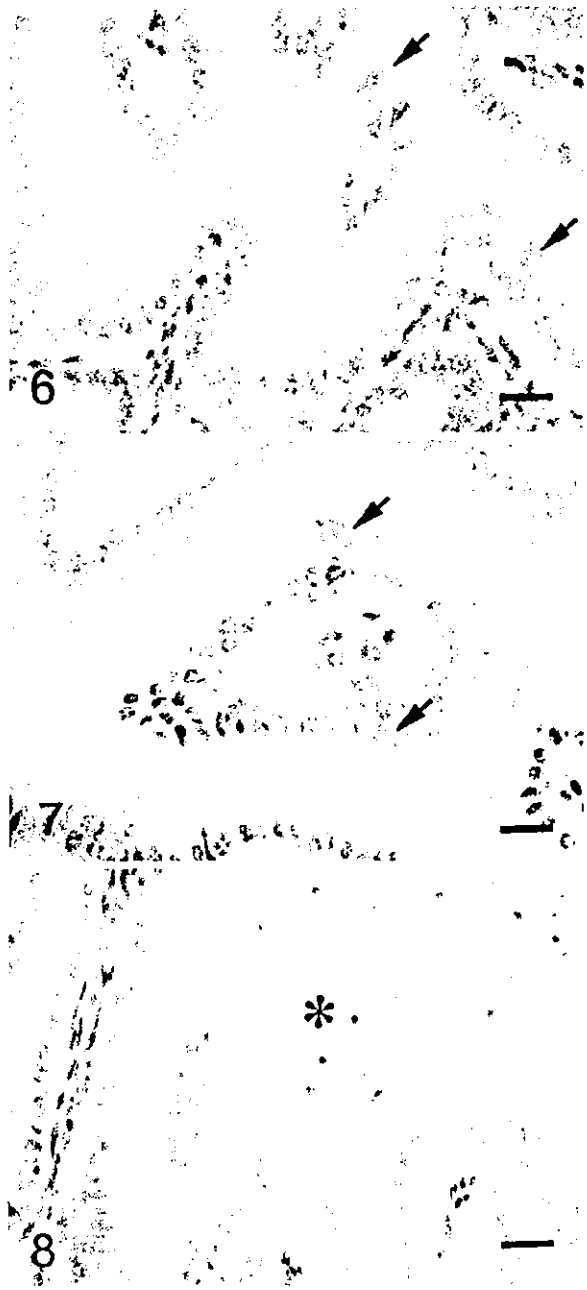

→

Fig. 6. Small intestine; mouse, 1 hour after inoculation with homogenized sheep brain with scrapie. GFAP signal is seen in the apical cytoplasm of enterocytes (*arrows*). ABC method, Mayer's hematoxylin counterstain. Bar = 20 mm.

Fig. 7. Small intestine; mouse, 1 hour after inoculation with homogenized sheep brain with scrapie. NF signal is observed in the apical and basilar cytoplasm of enterocytes (*arrows*). ABC method, Mayer's hematoxylin counterstain. Bar = 20 mm.

Fig. 8. Small intestine; mouse, 1 hour after inoculation with homogenized brain of normal sheep (*). No PrPc signal is seen in the cytoplasm of enterocytes. Tissues were subjected to multiple pretreatments. ABC method, Mayer's hematoxylin counterstain. Bar = 50 mm.

were incubated with primary antibodies at room temperature for 30 minutes. After washing with distilled water, sections were incubated with 0.5% biotinylated goat antirabbit antibody for 30 minutes at room temperature and with ABC conjugated peroxidase for 30 minutes. Color was developed in a 0.05% 3,3'-diaminobenzidine solution. Tissue sections without pretreatment were incubated with rabbit antibody to bovine glial fibrillary acidic protein (GFAP) (Dako, Co., Carpinteria, CA) and a rabbit antibody cocktail to human neurofilament (NF) (Affinity Research Products Limited, Mamhead, UK): these proteins served as markers of nervous tissue.

In the brain of the sheep with scrapie, cytoplasmic vacuolation of neurons and spongiform change of the gray matter were identified in the HE sections of the medulla oblongata.[13] Immunoreactivity for PrPc was found in the neuropil of the medulla oblongate (Fig. 1).

In the small intestine of all five mice given scrapie-affected brain 1 hour prior to being killed, sheep brain tissue was present in the gut lumen. Immunopositive signals for PrPc were found in the intralumenal sheep brain tissue (Fig. 2) and the apical and basilar cytoplasm of villus and crypt enterocytes (Fig. 3) in the small intestine of all mice treated with scrapie brain. When PrPc antibody was omitted, no positive signals for PrPc were found in enterocytes (Fig. 4). PrPc-positive cells ranged from 1 to 2 per high-power field (Fig. 5). Positive signals for GFAP and NF were found in the medulla oblongata of the sheep brain with scrapie and in enterocytes of the small intestine of all mice inoculated with scrapie brain (Figs. 6 and 7).

In all mice given normal brain, no PrPc was seen in the intralumenal brain tissue or enterocytes of the small intestine (Fig. 8), but signal for GFAP- and NF-positive signals was found in the enterocytes.

For immunohistochemical detection of abnormal PrPsc in the brain, several pretreatments have been employed, including picric acid, formic acid, steam autoclaving, and microwave treatment, because epitope retrieval after formalin fixation and paraffin embedding of the brain tissue is very difficult.[4] Without pretreatment there is a high probability of false-negative immunostaining.[4] Therefore, single or multiple pretreatments are necessary for immunohistochemical detection of the PrPsc. In the present study, we used multiple pretreatments. Immunopositivity for PrPc was detected in the sheep brain with scrapie and in enterocytes of mice inoculated with sheep brain containing the abnormal scrapie prion. The immunohistochemical results suggest entry of PrPsc into the cytoplasm of enterocytes. However, absorption of sheep brain containing PrPsc occurred only in enterocytes in the duodenum and jejunum in this study. Intralumenal sheep brain was observed only as far distally as the jejunum. This material could not be observed in the ileum in mice at only 1 hour after ingestion. Observation of absorbed PrPsc in the ileum would require being killed later. We have demonstrated absorption of PrPsc in the jejunum and ileum of adult mice in another study (M. Okamoto, T. Noguchi, and H. Tamiyama, unpublished data). It is not clear from our studies whether different segments of the small intestine differ in their ability to absorb the macromolecular proteins of sheep brain.

In Germany, milk substitutes made from bone meal and fat of diseased animals are believed to play an important role in the transmission of BSE in cattle.[8] In the present study, immunohistochemistry suggests that PrPsc of sheep brain affected by scrapie enters neonatal murine enterocytes by pinocytosis. Thus, the results support the possibility that PrPsc included in milk substitutes may be absorbed by enterocytes of the small intestine of the neonate and may thus be an important pathway for neonatal PrPsc transmission in sheep, cattle, and mice. The mechanism of PrPsc transmission from enterocytes to the germinal centers of lymphoid tissues or peripheral nerve systems remains unclear.

Acknowledgement

The present study was supported in part by a grant from Gakujutsu-Frontier cooperative research in Rakuno Gakuen University.

References

1 Barker LK, van Dreumel AA, Palmer N: The alimentary system. *In*: Pathology of Domestic Animals, ed. Jubb KVF, Kennedy PC, and Palmer N, 4th ed., vol. 2, pp. 74–83, Academic Press, New York, 1993

2 Beekes M, McBride PA: Early accumulation of pathological PrP in the enteric nervous system and gut-associated lymphoid tissue of hamsters orally infected with scrapie. Neurosci Lett **278**:181–184, 2000

3 Bueler H, Fischer M, Lang Y, Bluethmann H, Lipp HP, DeArmond SJ, Prusiner SB, Aguet M, Weissmann C: Normal development and behaviour of mice lacking the neuronal cell-surface PrP protein. Nature **356**:577–582, 1992

4 Everbroeck BV, Pals P, Martin JJ, Cras P: Antigen retrieval in prion protein immunohistochemistry. J Histochem Cytochem **47**:1465–1470, 1999

5 Ghosh S: Intestinal entry of prions. Z Gastroenterol **40**: 37–39, 2002

6 Horiuchi M, Yamazaki N, Ikeda T, Ishiguro N, Shinagawa M: A cellular form of prion protein (PrPc) exists in many non-neuronal tissues of sheep. J Gen Virol **76**: 2583–2587, 1995

7 Huang FP, Farquhar CF, Mabbott NA, Bruce ME, MacPherson GG: Migrating intestinal dendritic cells transport PrPSc from the gut. J Gen Virol **83**:267–271, 2002

8 Kamphues J, Zentek J, Oberthur RC, Flachowsky G, Coenen M: Animal-derived feeds as possible vectors for bovine spongiform encephalopathy (BSE) in Germany. 1. Comparative risk assessment for a single animal food of animal origin. Dtsch Tierarztl Wochenschr **108**:283–290, 2001

9 Maignien T, Lasmezas CI, Beringue V, Dormont D, Deslys JP: Pathogenesis of the oral route of infection of mice with scrapie and bovine spongiform encephalopathy agents. J Gen Virol **80**:3035–3042, 1999

10 McBride PA, Eikelenboom P, Kraal G, Fraser H, Bruce ME: PrP protein is associated with follicular dendritic cells of spleens and lymph nodes in uninfected and scrapie-infected mice. J Pathol **168**:413–418, 1992

11 Shinagawa M, Matsuda A, Sato G, Takeuchi M, Ichijo S, Ono T: Occurrence of ovine scrapie in Japan: clinical and histological findings in mice inoculated with brain homogenates of an affected sheep. Jpn J Vet Sci **46**:913–916, 1984
12 Takahashi H, Takahashi RH, Hasegawa H, Horiuchi M, Shinagawa M, Yokoyama T, Kimura K, Haritani M, Kurata T, Nagashima K: Characterization of antibodies raised against bovine-PrP peptides. J Neurovirol **5**:300–307, 1999
13 Taniyama H, Ichijo S, Ono T: The occurrence of scrapie of sheep in Japan. Jpn J Vet Sci **46**:741–744, 1984
14 Van Keulen LJ, Schreuder BE, Vromans ME, Langeveld JP, Smits MA: Scrapie-associated prion protein in the gastrointestinal tract of sheep with natural scrapie. J Comp Pathol **121**:55–63, 1999
15 Walker WA, Abel SN, Wu M, Bloch KJ: Intestinal uptake of macromolecules. V. Comparison of the vitro uptake by rat small intestine of antigen-antibody complexes prepared in antibody or antigen excess. J Immunol **117**: 1028–1032, 1976

Request reprints from Dr. H. Taniyama, Department of Veterinary Pathology, School of Veterinary Medicine, Rakuno Gakuen University, 582 Bunkyodai-Midorimachi, Ebetsu, Hokkaido 069-8501 (Japan). E-mail: taniyama@rakuno.ac.jp.

COMMUNICATION

OBC www.rsc.org/obc

Effects of β-sheet breaker peptide polymers on scrapie-infected mouse neuroblastoma cells and their affinities to prion protein fragment PrP(81–145)

Takehisa Oishi,[a] Ken-ichi Hagiwara,[b] Tomoya Kinumi,†[b] Yoshio Yamakawa,[b] Masahiro Nishijima,[b] Kazuhiko Nakamura[c] and Hirokazu Arimoto*[a,d]

[a] *Department of Chemistry, Graduate School of Science, Nagoya University, Chikusa, Nagoya 464-8602, Japan. E-mail: arimoto@org.chem.nagoya-u.ac.jp; Fax: +81-52-789-5041*

[b] *Department of Biochemistry and Cell Biology, National Institute of Infectious Diseases, Tokyo 162-8640, Japan*

[c] *Institute for Biological Resources and Functions, National Institute of Advanced Industrial Science and Technology, Tsukuba, Ibaraki 305-8566, Japan*

[d] *Institute for Advanced Research, Nagoya University; and PRESTO, JST, Chikusa, Nagoya 464-8602, Japan*

Received 16th June 2003, Accepted 3rd July 2003
First published as an Advance Article on the web 9th July 2003

The effects of Soto's 'β-sheet breaker peptide' and its polymer on PrP^{Sc} formation in ScN2a cells were investigated. Surface plasmon resonance study indicated that direct binding between PrP(81–145) and the 'β-sheet breaker peptide' is not specific and may not play a major role in the inhibition of PrP^{Sc} formation.

Introduction

Prions are transmissible, fatal neurodegenerative agents that affect humans and a wide variety of animals.[1] In the PRION-ONLY hypothesis, direct interaction between the pathogenic prion protein (PrP^{Sc}) and the endogenous cellular prion protein leads to PrP^{Sc} accumulation, which plays a central role in the transmissible spongiform encephalopathies (TSEs). PrP^{Sc} is an abnormally folded, protease-resistant, β-sheet-rich isoform of a normal protein PrP^{C}.

Molecules that stabilize the conformation of PrP^{C}, or destabilize PrP^{Sc} *via* specific binding, are currently targets of active investigations.

Several synthetic peptides,[2] and some low-molecular weight organic compounds,[3] have been reported to inhibit these transformations *in vitro*. Among these, Soto's β-sheet breaker peptide (i-PrP13: sequence DAPAAPAGPAVPV) (Fig. 1) blocks PrP^{Sc} formation in cell-free systems and scrapie-infected cell culture.[4] Intracerebral injection of i-PrP13 with infectious PrP^{Sc} also delays the time to the onset of symptoms for mice.[4] The mechanism of action, however, remains elusive.

i-PrP13 is a synthetic peptide that was designed based on the conserved residues 115–122 of prion proteins (sequence: AAAAGAVV). Aspartic acid and four prolines were inserted into the native sequence. The above region, PrP(115–122), has been suggested to play a central role in the conversion of PrP^{C} to PrP^{Sc}.[5] It has therefore been implied that a direct interaction of i-PrP13 with the prion protein at the conserved region is important to its inhibitory activities. This assumption, however, has not been examined experimentally.

We quantitatively measured the affinity of the 'β-sheet breaker' (i-PrP13) with PrP(81–145) by means of surface plasmon resonance (SPR). The dissociation constant K_D was fairly large (> 10^{-3} M), which provided evidence against the initial hypothesis.

We then devised and chemically synthesized an oligomeric i-PrP13 with enhanced affinity to PrP(81–145).

The inhibitory activities of both monomeric and oligomeric i-PrP13 were evaluated with the prion-infected mouse neuroblastoma ScN2a cell line.

Results

The SPR technique was applied to evaluate the affinity between i-PrP13 and a prion protein fragment PrP(81–145). First, mouse PrP(81–145) was prepared by solid-phase peptide synthesis (yield 23%). To produce an affinity toward anti-prion monoclonal antibody 3F4 (DAKO), residues 108 (L to M) and 111 (V to M) were replaced. ε-Biotinylated L-lysine and two glycines (as linkers) were added at the C-terminus so that the peptide could be immobilized to the SPR sensor tip surface. The sequence of the synthetic PrP(81–145) is shown in Fig. 2.

The molecular ion (*m/z* 7115.0 for M + H^+) for synthetic PrP(81–145), as observed by MALDI-TOF mass spectrometry, corresponds well with the calculated molecular weight (7114).

The biotinylated PrP(81–145) was injected over the gold surface coated with streptavidin (Sensor tip SA, BIAcore). A surface density of 4000 resonance units was generated for PrP(81–145), which corresponds to approximately 4 ng mm^{-2}.

Differing amounts of PrP-specific monoclonal antibody 3F4 were applied to the biosensor immobilizing PrP(81–145) (Fig. 3). An analysis of these sensorgrams gave a dissociation constant K_D of 7.0×10^{-9} M. This result corresponded well

† Human Stress Signal Research Center, National Institute of Advanced Industrial Science and Technology, Ikeda, Osaka 563-8577, Japan.

DOI: 10.1039/b306682g

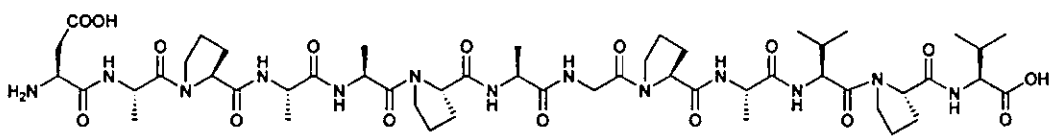

Fig. 1 'β-Sheet breaker peptide' (i-PrP13) 1.

81 GQPHGGGWGQGGGTHNQWNKPSKPKTNMKH 110

111 MAGAAAAGAVVGGLGGYMLGSAMSRPMIHF 140

141 GNDWEGGK(biot)

Linker

Fig. 2 Biotinylated mouse PrP(81–145).

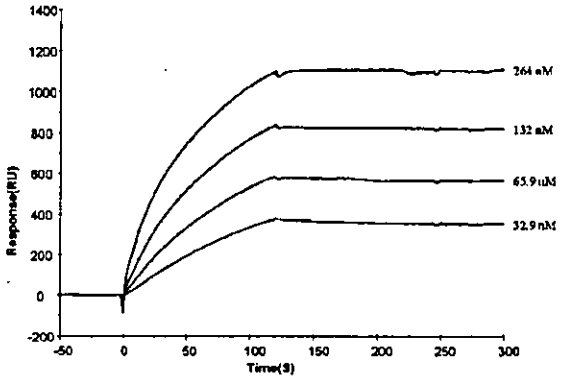

Fig. 3 SPR sensorgrams of anti-prion monoclonal antibody 3F4 binding to immobilized mouse PrP(81–145).

with the reported value of K_D 2.15 × 10^{-8} M between Syrian hamster PrP(29–231) and 3F4,[6] which validated the sensor tip for detection of specific binding to PrP.

However, there was no interaction detected when the β-sheet breaker i-PrP13 was employed as an analyte (K_D > 10^{-3} M, sensorgrams are not shown).

The results were in conflict with the widely circulated hypothesis that i-PrP13 has specific affinity to PrP. This unexpected finding prompted us to synthesize a polymer of i-PrP13 to provide insight into binding affinity–inhibitory relationships.

Cluster effects or multi-valent effects are molecular design principles that enhance weak nonbonding interactions.[7] Thus, a polymer of i-PrP13 would have higher affinity to PrP by these effects. This strategy has been very popular in sugar science, and we successfully utilized this approach in a glycopeptide antibiotic vancomycin, where both the affinity to their receptors and the antibacterial activities against resistant bacteria were significantly improved.[8]

The side-chain amino group of L-lysine was modified with a norbornene subunit, and the modified amino acid K(norbornene) was then introduced at the N-terminal (Scheme 1) or C-terminal portion of i-PrP13 (not shown).

Ring-opening polymerization of the peptide was performed using Grubbs catalyst[9] in chloroform–methanol (1 : 1). Fmoc groups of the resulting polymer were removed with piperidine.

The SPR sensorgram of the N-terminally-modified i-PrP13 polymer **3** is shown in Fig. 4.[10] Unlike monomeric i-PrP13, the polymer had specific interactions with immobilized PrP(81–145). Because the rigorous analysis of data was not trivial due to the polyvalent nature of the sample, the apparent dissociation constant K_D was estimated on a per monomer-unit basis. The K_D value of 1.91 × 10^{-4} M indicated an at least 10-fold enhancement of affinity.

We investigated next if the i-PrP13 or its polymers inhibited the accumulation of PrP^{Sc} in scrapie-infected mouse neuroblastoma N2a cell (ScN2a), following the procedures of Prusiner *et al.*[11]

The 1 μM of quinacrine was used as a positive control.

It was proved that neither the i-PrP13 (lane 2) nor the polymers (lanes 4, 6) inhibited the formation of proteinase K resistant PrP^{Sc} up to 250 μg ml^{-1} (Fig. 5). In contrast, the

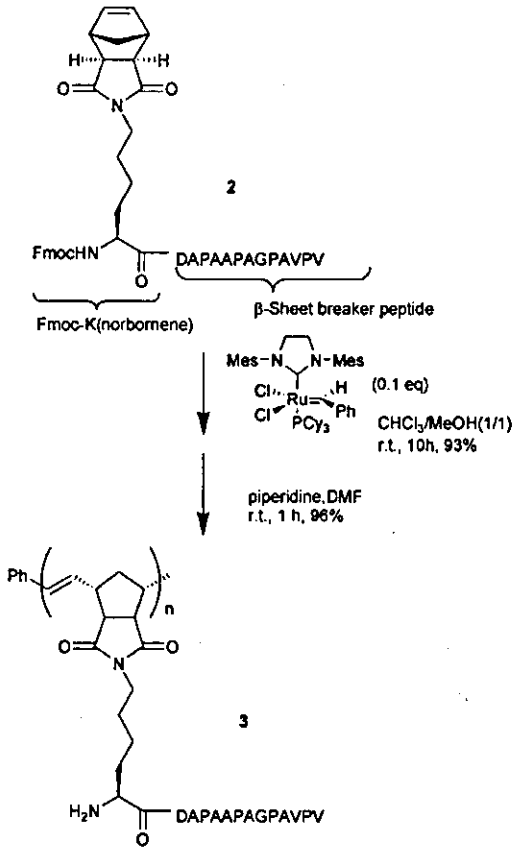

Scheme 1 Synthesis of i-PrP-polymer (average n = 10).

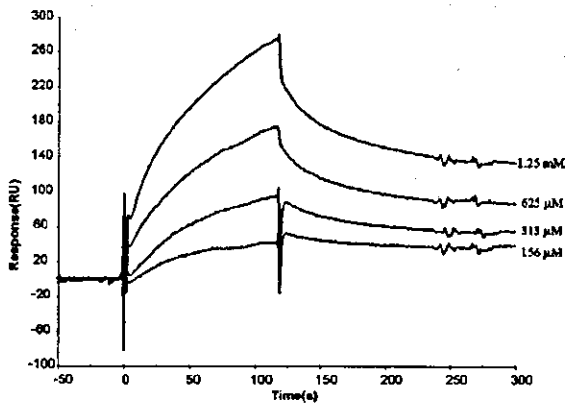

Fig. 4 SPR sensorgrams of an i-PrP13 polymer 3 binding to immobilized mouse PrP(81–145).

positive control (quinacrine) effectively cleared the formation of PrP^{Sc} at a concentration of 1 μM. Because we and Soto *et al.* have employed different cells for our cell-culture studies, a direct comparison of data is not possible. However, the inhibitory activity of i-PrP13 was much weaker than that of quinacrine.[12]

Discussion

Conversion to the infectious conformer PrP^{Sc} is particularly associated with major structural rearrangement in the central portion of the prion protein. PrP(90–145) is the region suggested to be the most important. Employing PrP-specific monoclonal antibodies with different epitope recognitions, Prusiner *et al.* have shown that the Fabs D13 (epitope: 132–156

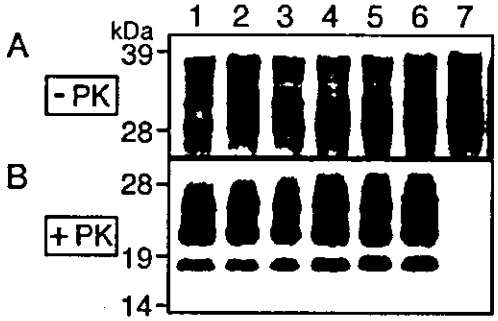

Fig. 5 Effects of i-PrP13 and its polymer on PrP^{Sc} formation of ScN2a cells—ScN2a cells were cultured for 5 days in the medium containing either unmodified i-PrP13 (lane 2), the N-terminally K(norbornene)-modified monomer (lane 3) and polymer (lane 4), or the C-terminally K(norbornene)-modified monomer (lane 5) and polymer (lane 6). As controls, the cells were grown in the absence of the peptides (lane 1) or in the presence of quinacrine (lane 7). The cell lysates were subjected to Western blotting analysis before (panel A) or after (panel B) proteinase K (PK) digestion.

of PrP) and D18 (epitope: 95–103 of PrP) only inhibit the formation of PrP^{Sc}. All PrP-specific antibodies have dissociation constants in the 10^{-9} M range. This result also suggests the importance of the central region.[13]

If the i-PrP13 specifically binds and stabilizes the normal conformation of prion proteins as hypothesized, it would likely inhibit their conversion to misfolded isoforms.

We have demonstrated in the present study, however, that i-PrP13 and even its polymer have poor specific interactions (dissociation constants of $> 10^{-3}$ M and 1.9×10^{-4} M, respectively) with the prion protein fragment PrP(81–145). In addition, they do not inhibit PrP^{Sc} accumulation in ScN2a cells at a high sample concentration of 250 μg ml^{-1}. These results indicate that direct binding of i-PrP13 might not play a major role in the inhibition of PrP^{Sc} formation. Although more investigation is needed, it is noteworthy that i-PrP13 did not show any inhibitory activities with regard to PrP^{Sc} formation in ScN2a cell lines, which is one of the most widely used cells in prion research. Our results provide the basis for mechanistic considerations of the effects of i-PrP13 peptide in an *in vivo* system.[4]

Experimental

General procedures for solid-phase peptide synthesis

The peptides employed in this study were synthesized by the conventional Fmoc solid-phase method with a Pioneer automated peptide synthesizer (Applied Biosystems). HATU was the coupling agent. 2-Cl-trityl chloride resin (Nova) was employed as a solid support so that the products were cleaved under mild conditions (acetic acid, trifluoroethanol). For the preparation of PrP(81–145), PAC-PEG-PS resin (Applied Biosystems) was employed. Acidic cleavage (TFA) of the PrP peptide from resin was conducted with scavengers (thiophenol and ethanedithiol).

Amino acids, including α-Fmoc-ε-biotinyl-L-lysine, were purchased from Watanabe Chemicals, Japan.

Synthetic peptides were purified by size-exclusion chromatography (Superdex 75HR 10/30, 30% aq. acetonitrile with 0.1% TFA).

Molecular ion peaks for all synthetic peptides were detected with a Voyager STR MALDI-TOF mass spectrometer (Applied Biosystems).

Norbornene-modified L-lysine [K(norbornene)]:

N-ε-Norbornene-modified L-lysine was synthesized according to Scheme 2.

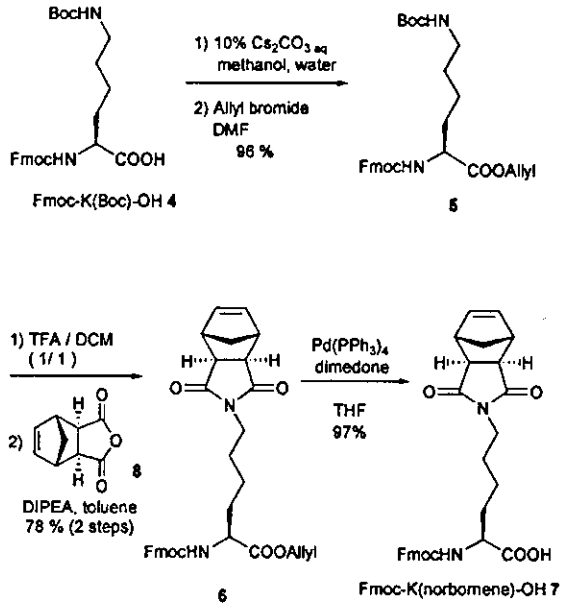

Scheme 2 Synthesis of Fmoc-K (norbornene)-OH.

β-Sheet breaker polymer

The N-terminally-modified monomer peptide **2** (sequence: Fmoc-K(norbornene)-DAPAAPAGPAVPV) was synthesized by the Fmoc method as described in the general procedures (total yield 87%). To a solution of the monomer in methanol–chloroform (1 : 1) was added a 0.1 equivalent of Grubbs catalyst to conduct ROMP (ring-opening metathesis polymerization). The degree of polymerisation was estimated as 10-mer. An Fmoc group of the product was removed with piperidine–DMF (4 : 1). The crude product was purified by size-exclusion chromatography. The poly-β-sheet breaker **3** proved to be fairly soluble in water (>> 5% wt/vol).

The C-terminally-modified polymer was also prepared by similar procedures.

Surface plasmon resonance (SPR)

Surface plasmon resonance was recorded with BIAcoreX (BIAcore), and the data were analyzed with BIAevaluation e.2 SPR kinetic software (BIAcore).

Solutions of the interacting peptide ('analyte') were injected over the surface at 25 °C with a flow rate of 10 μL min^{-1} in HBS running buffer [10 mM Hepes (pH 7.4)–150 mM NaCl, 3 mM EDTA, 0.005% (v/v) Surfactant P20]. After injection, analyte solutions were replaced by HBS at the same flow rate. The surface was regenerated with 5 mM glycine (pH 2.0, 30 s, 10 μL) after each measurement. Analyte solutions were run simultaneously over a control surface without immobilized PrP(81–145). The response in the control flow cell was subtracted from each sensorgram, and the sensorgram was normalized to a baseline of 0 RU.

In vitro assay for PrP^{Sc} formation

ScN2a cells were cultured in Dulbecco's Modified Eagle Medium (GIBCO™) supplemented with fetal calf serum (10%), penicillin (50 unit ml^{-1}), and streptomycin (50 μg ml^{-1}). i-PrP13 or its K(norbornene)-derivatives at a final concentration of 250 μg ml^{-1} (equivalent to 1.7×10^{-4} M i-PrP13 monomer) were added to the the cells grown in 25 cm^3 flasks (day 1). To overcome the problem of possible extracellular and/or intracellular degradation of the peptides, supplementary doses (a final concentration of 100 μg ml^{-1}) of the peptides were added to the

medium on day 3. As controls, the cells were grown in the absence of compounds or in the presence of 1 μM quinacrine. The cells were harvested on day 5 and subjected to the proteinase K digestion assay to determine the amounts of PrP^{Sc} by Western blotting utilizing anti-PrP antibody 6H4 (Prionics).[11]

Acknowledgements

We thank Professor Daisuke Uemura (Nagoya University) for helpful discussions and support, and Dr Kiyotoshi Kaneko (National Institute of Neuroscience, Tokyo) for providing ScN2a cells. We acknowledge a Grant-in-Aid for Scientific Research from the Ministry of Education, Science, Sports and Culture, Japan (No. 12558076), and the Uehara Memorial Foundation for financial support.

Notes and references

1 G. C. Telling et al., *Science*, 1996, **274**, 2079; S. B. Prusiner, *Proc. Natl. Acad. Sci. U. S. A.*, 1998, **95**, 13363 . For a recent review: A. Aguzzi, M. I. Glatzel, F. Montrasio, M. Prinz and F. L. Heppner, *Nat. Rev. Neurosci.*, 2001, **2**, 745.

2 K. Kaneko, D. Peretz, K. Pan, T. C. Blockberger, H. Wille, R. Gabizon, O. H. Griffith, F. E. Cohen, M. A. Baldwin and S. B. Prusiner, *Proc. Natl. Acad. Sci. U. S. A.*, 1995, **92**, 11160; K. Kaneko, H. Wille, I. Mehlhorn, H. Zhang, H. Ball, F. E. Cohen, M. A. Baldwin and S. B. Prusiner, *J. Mol. Biol.*, 1997, **270**, 574.

3 B. Caughey and R. E. Race, *J. Neurochem.*, 1992, **59**, 768; M. Pocchiari, S. Schmittinger and C. Masullo, *J. Gen. Virol.*, 1987, **68**, 219; S. P. Priola, A. Raines and W. S. Caughey, *Science*, 2000, **287**, 1503.

4 C. Soto, R. J. Kascsak, G. P. Saborio, P. Aucouturier, T. Wisniewski, F. Prelli, R. Kascsak, E. Mendez, D. A. Harris, J. Ironside, F. Tagliavini, R. I. Carp and B. Frangione, *Lancet*, 2000, **355**, 192.

5 L. De Gioia, C. Selvaggini, E. Ghibaudi, L. Diomede, O. Bugiani, G. Forloni, F. Tagliavini and M. Salmona, *J. Biol. Chem.*, 1994, **269**, 7859; H. Zhang, K. Kaneko, J. T. Nguyen, T. L. Livshits, M. A. Baldwin, F. E. Cohen, T. L. James and S. B. Prusiner, *J. Med. Biol.*, 1995, **250**, 514; J. Chabry, B. Caughhey and B. Chesebro, *J. Biol. Chem.*, 1998, **273**, 13203.

6 E. Leclerc, D. Peretz, H. Ball, H. Sakurai, G. Legname, A. Serban, S. B. Prusiner, D. R. Burton and R. A. Williamson, *EMBO J.*, 2001, **20**, 1547.

7 M. Mammen, S. K. Choi and G. M. Whitesides, *Angew. Chem., Int. Ed.*, 1998, **37**, 2754.

8 H. Arimoto, K. Nishimura, T. Kinumi, I. Hayakawa and D. Uemura, *Chem. Commun.*, 1999, 1361; H. Arimoto, T. Oishi, M. Nishijima and T. Kinumi, *Tetrahedron Lett.*, 2001, **42**, 3347.

9 M. Scholl, S. Dinf, C. W. Lee and R. H. Grubbs, *Org. Lett.*, 1999, **1**, 953; A. K. Chatterjee, J. P. Morgan, M. Scholl and R. H. Grubbs, *J. Am. Chem. Soc.*, 2000, **122**, 3783.

10 C-Terminally-K(norbornene)-modified-monomer and its polymer were poorly soluble in water; an affinity analysis was therefore not conducted.

11 K. Doh-ura, T. Iwaki and B. Caughey, *J. Virol.*, 2000, **74**, 4894; C. Korth, B. C. H. May, F. E. Cohen and S. B. Prusiner, *Proc. Natl. Acad. Sci. U. S. A.*, 2001, **98**, 9836.

12 Other nonpeptidic inhibitors have exhibited excellent activities in this assay. For example, quinacrine has been reported to have an EC_{50} of 0.3 μM: see ref. 11.

13 S. B. Prusiner, D. Peretz, R. A. Williamson, K. Kaneko, J. Vergara, E. Leclerc, G. Schmitt-Ulms, I. R. Mehlhorn, G. Legname, M. R. Wormald, R. M. Rudd, R. A. Dwek and D. R. Burton, *Nature*, 2001, **412**, 739.

Jpn. J. Infect. Dis., 56, 2003

Laboratory and Epidemiology Communications

Atypical Proteinase K-Resistant Prion Protein (PrP^{res}) Observed in an Apparently Healthy 23-Month-Old Holstein Steer

Yoshio Yamakawa*, Ken'ichi Hagiwara, Kyoko Nohtomi, Yuko Nakamura, Masahiro Nishijima, Yoshimi Higuchi[1], Yuko Sato[1], Tetsutaro Sata[1] and the Expert Committee for BSE Diagnosis, Ministry of Health, Labour and Welfare of Japan[2]

Department of Biochemistry & Cell Biology and
[1]Department of Pathology, National Institute of Infectious Diseases, Tokyo 162-8640 and
[2]Ministry of Health, Labour and Welfare, Tokyo 100-8916

Communicated by Tetsutaro Sata

(Accepted December 2, 2003)

Since October 18, 2001, 'bovine spongiform encephalopathy (BSE) examination for all cattle slaughtered at abattoirs in the country' has been mandated in Japan by the Ministry of Health, Labour and Welfare (MHLW). 'Plateria' ELISA-kit (Bio-Rad Laboratories, Hercules, Calif., USA) is routinely used at abattoirs for detecting proteinase K (PK)-resistant prion protein (PrP^{Sc}) in the obex region. Samples positive according to the ELISA screening are further subjected to Western blot (WB) and histologic and immunohistochemical examination (IHC) at the National Institute of Infectious Diseases (NIID) or Obihiro University. If PrP^{Sc} is detected either by WB or by IHC, the cattle are diagnosed as BSE. The diagnosis is approved by the Expert Committee for BSE Diagnosis, MHLW. From October 18, 2001 to September 30, 2003, approximately 2.5 million cattle were screened at abattoirs. A hundred and ten specimens positive according to ELISA were subjected to WB/IHC. Seven showed positive by both WB and IHC, all exhibiting the typical electrophoretic profile of a high content of the di-glycosylated molecular form of PrP^{Sc} (1-3) and the distinctive granular deposition of PrP^{Sc} in neuronal cells and neuropil of the dorsal nucleus of vagus.

An ELISA-positive specimen from a 23 month-old Holstein steer slaughtered on September 29, 2003, in Ibaraki Prefecture (Ibaraki case) was sent to the NIID for confirmation. The animal was reportedly healthy before slaughter. The OD titer in ELISA was slightly higher than the 'cut-off' level given by the manufacturer. The histology showed no spongiform changes and IHC revealed no signal of PrP^{Sc} accumulation typical for BSE. However, WB analysis of the homogenate that was prepared from the obex region and used for ELISA revealed a small amount of PrP^{Sc} with an electrophoretic profile different from that of typical BSE-associated PrP^{Sc} (1-3). The characteristics were (i) low content of the di-glycosylated molecular form of PrP^{Sc}, (ii) a faster migration of the non-glycosylated form of PrP^{Sc} on SDS-PAGE, and (iii) less resistance against PK digestion as compared with an authentic PrP^{Sc} specimen derived from an 83-month-old Holstein (Wakayama case) (Fig. 1). Table 1 summarizes the relative amounts of three distinctive glycoforms (di-, mono, non-glycosylated) of PrP^{Sc} calculated by densitometric analysis of the blot shown in Fig. 1. As 2.5 mg wet weight obex-equivalent homogenate of the Ibaraki case (Fig. 1, lane 4) gave slightly stronger band intensities of PrP^{Sc} than an 8 μg wet weight obex-equivqlent homogenate of a typical BSE-affected Wakayama case (Fig. 1, lane 2), the amount of PrP^{Sc}

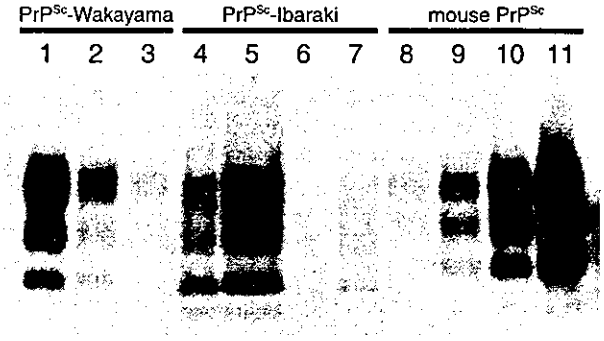

Fig. 1. Western blot analysis of PrP^{Sc} after proteinase K digestion. Lanes 1-3: typical bovine PrP^{Sc} obtained from Wakayama case (32, 8 and 2 μg tissue equivalent). Lanes 4 and 5: Ibaraki case PrP^{Sc} (2.5 and 10 mg tissue equivalent). Lanes 6 and 7: Ibaraki case PrP^{Sc} after additional proteinase K (PK) digestion (2.5 and 10 mg tissue equivalent). Lanes 8-11: mouse PrP^{Sc} (0.1, 0.4, 1.5 and 6 μg tissue equivalent). Western blot analysis was performed according to the protocol recommended by the Expert Committee for BSE Diagnosis, MHLW. Briefly, 50 mg of brain tissue was hydrolyzed successively with collagenase (50 μg/ml, for 30 min) and PK (40 μg/ml, for 30 min) at 37°C in 500 μl of 50 mM Tris-HCl buffer (pH 7.5) containing 0.1 M NaCl, 2% zwittergent 3-14, 0.5% sarcosyl and 5% 2-butanol. After PK was inhibited by the addition of Pefa-block (2 mM), the homogenate was hydrolyzed with DNase I (40 μg/ml) for 5 min at room temperature. PrP^{Sc} was then precipitated by the addition of 250 μl of 2-butanol-methanol mixture (5:1, v:v) and centrifugation at 15,000 rpm for 15 min. The precipitates were dissolved with 50 μl of the SDS-sample buffer and SDS-PAGE (12% polyacrylamide gel was applied) (lanes 1-5 and 8-11). Alternatively, the precipitates thus obtained were subjected to the second round of PK digestion before applying to SDS-PAGE (lanes 6, 7). Proteins were transferred onto PVDF membrane and PrP^{Sc} was detected by a mouse monoclonal antibody 44B1 (mAb 44B1), which recognizes a discontinuous epitope located between 155 and 231 amino acids in the mouse PrP sequence (Kim, C-L. et al., Virology, in press), and horse-radish peroxidase-labeled anti-mouse IgG for ECL-chemiluminescence (Amersham, Buckinghamshire, UK) detection. Upon the WB described above, PrP^{Sc} contained in as small as 1-2 μg brain tissues (obex or thalamus) of BSE affected cattle (lane 3) and PrP^{Sc} in 0.1 μg brain tissue of terminally sick mice (lane 6) were detectable.

*Corresponding author: Mailing address: Department of Biochemistry and Cell Biology, National Institute of Infectious Diseases, Toyama 1-23-1, Shinjuku-ku, Tokyo 162-8640, Japan. Tel: +81-3-5285-1111, Fax: +81-3-5285-1157, E-mail: yamakawa@nih.go.jp

Table 1. Comparison of the glycoform ratio between typical and atypical PrP^{Sc}

Molecular species in PrP^{Sc}	Ratio of the band intensity (%)	
	Wakayama case (typical case)	Ibaraki case (atypical case)
Di-glycosylated PrP^{Sc}	69.3	47.6
Mono-glycosylated PrP^{Sc}	23.2	26.5
Non-glycosylated PrP^{Sc}	7.5	25.9

The band intensities of the non-, mono-, and di-glycosylated forms of PrP^{Sc} of the Wakayama and Ibaraki cases (Fig. 1, lanes 1 and 5) were determined by a digital-image analysis software (Image Gauge, version 3.45, Fuji Photo Film Co., Tokyo), and the ratio of the three glycoforms were calculated.

accumulated in the Ibaraki case was calculated to be 1/500-1/1000 of the Wakayama case. In the Ibaraki case, the PrP^{Sc} bands were not detectable in the homogenates of the proximal surrounding region of the obex. These findings were consistent with the low OD value in ELISA, i.e., 0.2-0.3 for the Ibaraki case versus over 3.0 for the Wakayama case. The DNA sequence of the PrP coding region of the Ibaraki case was the same as that appearing in the database (GenBank accession number: AJ298878). More recently, we encountered another case that resembled the Ibaraki case. It was a 21-month-old Holstein steer from Hiroshima Prefecture. WB showed typical BSE-specific PrP^{Sc} deposition though IHC did not detect positive signals of PrP^{Sc} (data not shown).

Though the clinical onset of BSE is usually at around 5 years of age or later, a 20-month-old case showing the clinical signs has been reported (4). Variant forms of BSE similar to our cases, i.e., with atypical histopathological and/or biochemical phenotype, have been recently reported in Italy (5) and in France (6). Such variant BSE was not associated with mutations in the prion protein (PrP) coding region as in our case (5,6).

The Ministry of Agriculture, Forestry and Fisheries of Japan (MAFF) announced a ban of feeding ruminants with meat bone meal (MBM) on September 18, 2001, and a complete ban was made on October 15 of the same year. According to the recent MAFF report, the previous seven cases of BSE in Japan were cattle born in 1995-1996 and possibly fed with cross-contaminated feed. However, the two cattle in this report were born after the complete ban. Whether contaminated MBM was implicated in the present cases remains to be investigated.

REFERENCES

1. Collinge, J., Sidle, K. C. L., Meads, J., Ironside, J. and Hill, A. F. (1996): Molecular analysis of prion strain variation and the aetiology of 'new variant' CJD. Nature, 383, 685-690.
2. Bruce, M. E., Will, R. G., Ironside, J. W., McConnell, I., Drummond, D., Suttie, A., McCardle, L., Chree, A., Hope, J., Birkett, C., Cousens, S., Fraser, H. and Bostock, C. J. (1997): Transmissions to mice indicate that 'new variant' CJD is caused by the BSE agent. Nature, 389, 498-501.
3. Hill, A. F., Desbruslais, M., Joiner, S., Sidle, K. C. L., Gowland, I. and Collinge, J. (1997): The same prion strain causes vCJD and BSE. Nature, 389, 448-450.
4. Matravers, W., Bridgeman, J. and Smith, M.-F. (ed.) (2000): The BSE Inquiry. p. 37. vol. 16. The Stationery Office Ltd., Norwich, UK.
5. Casalone, C., Zanusso, G., Acutis, P. L., Crescio, M. I., Corona, C., Ferrari, S., Capobianco, R., Tagliavini, F., Monaco, S. and Caramelli, M. (2003): Identification of a novel molecular and neuropathological BSE phenotype in Italy. International Conference on Prion Disease: from basic research to intervention concepts. Gasreig, München, October 8-10.
6. Bicaba, A. G., Laplanche, J. L., Ryder, S. and Baron, T. (2003): A molecular variant of bovine spongiform encephalopatie. International Conference on Prion Disease: from basic research to intervention concepts. Gasreig, München, October 8-10.
7. Asante, E. A., Linehan, J. M., Desbruslais, M., Joiner, S., Gowland, I., Wood, A. L., Welch, J., Hill, A. F., Lloyd, S. E., Wadsworth, J. D. F. and Collinge, J. (2002). BSE prions propagate as either variant CJD-like or sporadic CJD-like prion strains in transgenic mice expressing human prion protein. EMBO J., 21, 6358-6366.

ELSEVIER

Journal of Immunological Methods 280 (2003) 157–164

JIM
Journal of
Immunological Methods

www.elsevier.com/locate/jim

Recombinant Technology

Two expression vectors for the phage-displayed chicken monoclonal antibody

Naoto Nakamura, Mariko Shimokawa, Kazuyoshi Miyamoto, Shintaro Hojyo, Hiroyuki Horiuchi, Shuichi Furusawa, Haruo Matsuda*

Laboratory of Immunobiology, Department of Molecular and Applied Biosciences, Graduate School of Biosphere Sciences, Hiroshima University, 1-4-4 Kagamiyama, Higashi, Hiroshima 739-8528, Japan

Received 28 August 2002; received in revised form 15 January 2003; accepted 11 April 2003

Abstract

We previously reported the development of chicken monoclonal antibodies (mAb) against mammalian-conserved molecules by cell fusion and phage display using the mouse mAb expression vector pPDS. However, chicken hybridomas produce relatively small amounts of antibody when compared with mouse hybridomas, and application of the pPDS may be limited in two-antibody assays with a mouse mAb because it contains mouse Cκ as a detection tag. To circumvent the above problems, two expression vectors were established and used to produce a functional recombinant chicken mAb. These vectors, which were designed to accommodate a single chain fragment of the variable region (scFv) of the antibody, contained a chicken Cλ and FLAG with or without 6 × histidine sequences in the 3′ terminus of the scFv to serve as detection and purification tags. In this study, a prion protein (PrP)-specific chicken mAb (HUC2-13) was expressed as phage-displayed and soluble scFv mAb forms by using these vectors. The scFv mAbs expressed by these vectors exhibited the same antigen-binding specificity to PrP as that of the original HUC2-13, could be purified with ease, and used in combination with a mouse mAb. These results indicate that the methods described herein offer an alternative to chicken mAb production from hybridomas and immunized chicken splenocytes, and may contribute to the use of chicken mAb reagents in numerous fields.

Keywords: Chicken monoclonal antibodies; Cell fusion; Phage display; Expression vectors

1. Introduction

The use of monoclonal antibodies (mAbs) has contributed greatly to progress in the biological and clinical sciences. However, conserved mammalian molecules are known to be less immunogenic in the mammals commonly used for immunization (Song et al., 1985; Groschup et al., 1997). The chicken is a useful animal for the development of specific antibodies against these proteins (Asaoka et al., 1992; Matsushita et al., 1998) as it is located on a different

Abbreviations: scFv, single chain fragment of the variable region; mAb, monoclonal antibody; VH, variable region of the heavy chain; Vλ, variable region of the light chain; PrP, prion protein; CHB, reverse primer for heavy chain variable region; CHSF, forward primer for heavy chain; CLSB, reverse primer for λ chain; CLF, forward primer for λ chain; CRB, reverse primer for reamplification of scFv fragment.

* Corresponding author. Tel./fax: +81-824-24-7968.
E-mail address: hmatsu@hiroshima-u.ac.jp (H. Matsuda).

0022-1759/$ - see front matter © 2003 Elsevier B.V. All rights reserved.
doi:10.1016/S0022-1759(03)00204-7

branch of the phylogenetic tree from mammals. We recently developed a chicken mAb named HUC2-13 that recognizes the N-terminal residues of the mammalian prion protein (PrP), which was generated by cell fusion (Matsuda et al., 1999). Although HUC2-13 is a very useful antibody in prion research, the hybridoma produces a small amount of antibody when compared with mouse hybridomas (Nishinaka et al., 1996). The rapid purification of chicken antibodies is sometimes difficult because chicken antibodies do not combine with protein A or protein G (Hadge and Ambrosius, 1984) and are more sensitive to acid or alkali treatment than are mammalian antibodies (Shimizu et al., 1992). In order to obtain a large quantity of the mAb, recombinant HUC2-13 scFv mAb was generated using the expression vector pPDS, as previously described (Nakamura et al., 2000). The recombinant mAb was reactive with PrP. These results indicate that the phage-display system is an effective antibody production tool and may replace the chicken hybridoma system. However, application of the pPDS vector is limited in two-antibody assay systems using a mouse mAb because it contains only the mouse Cκ sequence as a detection tag (Yamanaka et al., 1995, 1996).

In this study, in order to overcome the above problems and enable the recombinant antibody to be used as a chicken antibody, we attempted to establish expression vectors optimized for chicken antibodies. We first constructed a new expression vector, which included chicken Cλ and FLAG sequences (Brizzard et al., 1994) in the 3′ terminus of the single chain fragment of the variable region (scFv) as detection tags. Secondly, a vector which had a 6 × histidine tag in the 3′ side of the FLAG sequence was also constructed in order to facilitate purification without an acidic buffer. Here, we show the usefulness of these two vectors in a chicken recombinant antibody system.

2. Materials and methods

2.1. Chicken hybridoma line

The chicken hybridoma cells HUC2-13 (Matsuda et al., 1999) were used because they produce an antibody specific to the N-terminal sequence (amino acids; RPKPG) of PrP. Cells were maintained in Iscove's modified Dulbecco's medium (Gibco, USA) containing 10% fetal bovine serum (Sigma, USA), in a 5% CO_2 incubator at 38.5 °C.

2.2. Antigen

The synthetic human PrP peptide (H25, amino acid residues; 25–49), as the HUC2-13-reactive antigen, was synthesized by solid-phase peptide synthesis (Model PSSM-8, Shimadzu, Japan). A 10% homogenate of normal BALB/c mouse brain was also used as intact PrP. Preparation was performed as previously described (Nishida et al., 2000).

2.3. RT-PCR

Total RNA was extracted from the HUC2-13 hybridoma cells (3.0×10^7 cells) with ISOGEN-LS (Nippon Gene, Japan). The first strand cDNA was primed with Oligo-$(dT)_{12-18}$ primer (Roche Diagnostics, Switzerland) and synthesized with a Superscript II Synthesis cDNA Kit (Gibco). The variable regions of the antibody were amplified by PCR with KOD plus DNA polymerase (Toyobo, Japan) using two primer pairs: CHB (forward), 5′-CTGATGGCGGCCGTGACGTT-3′, containing an *Eag*I restriction site (underlined) and CHSF (reverse), 5′-TCCACCTGTCGACACGATGACTTCGGT-3′ for the amplification of the variable heavy chain (VH), CLSB (forward), 5′-TCTGACGTCGCGCTGACTCAGCC-3′ and CLF (reverse), 5′-CTTGGGCGCGCCTAGGACGGTCAGGGTT-3′, containing a *Bss*HII restriction site (underlined) for the amplification of the variable λ-light chain (Vλ). The scFv linker was prepared as previously described (Yamanaka et al., 1995, 1996). In order to make the scFv fragment, purified VH and Vλ fragments were assembled with purified scFv linker by PCR. Re-amplification of the scFv was performed using CRB, 5′-TATCTGATGGCGGCCGTGA-3′, containing an *Eag*I restriction site (underlined) and CLF primers.

2.4. Construction of pCPDS and His-pCPDS vectors

Chicken Cλ-cDNA was obtained from H-B15 inbred chicken cDNA cloned into pBluescriptII SK (−) (Stratagene, USA) by PCR. For overlapping

PCR, the chicken Cλ sequence cloned into pBluescriptII SK (–) was re-amplified using another primer pair, the forward primer containing *Eag*I and *Bss*HII restriction sites, and the reverse containing the amber stop codon and FLAG sequence (amino acids; DYKDDDDK). The 3′ half of gene III was amplified from the pPDS vector using a forward primer including the amber stop codon and a part of the FLAG sequence, and a reverse primer containing an *Eco*RI site. They were assembled by the overlapping PCR method and then cut by *Eag*I and *Eco*RI. These enzyme-treated constructs were ligated to the identically treated pPDS, and the final constructed vector was named pCPDS.

To introduce the 6 × histidine tag into pCPDS, the chicken Cλ and FLAG sequences were amplified from the pCPDS vector using a forward primer (Cλ re-amplification primer) and a reverse primer containing the amber stop codon, the 6 × histidine tag and the FLAG sequence. The 3′ half of gene III was amplified from the pCPDS vector using a forward primer containing the 6 × histidine tag and gene III sequences, and a reverse primer (gene III amplification primer). They were assembled using the overlapping PCR method and then cut with *Eag*I and *Eco*RI. These enzyme-treated constructs were ligated to the identically treated pPDS, and the final constructed vector was named His-pCPDS.

2.5. Construction of the scFv antibody

Fifty nanograms of the HUC2-13 scFv fragment was ligated with 100 μg of pCPDS or His-pCPDS at the *Eag*I and *Bss*HII sites. The resulting DNA was transformed into 100 μl aliquots of *Escherichia coli* XL1-Blue competent cells (Stratagene), and then plated on LB agar (13 g/l of Bacto agar, 10 g/l of tryptone, 5 g/l of yeast extract, and 10 g/l of NaCl) supplemented with 100 μg/ml of ampicillin. The culture was then infected with VCS-M13 (7.5×10^9 PFU, Stratagene) in a medium containing ampicillin (100 μg/ml), tetracycline (50 μg/ml) and 1% glucose. Cells were collected by centrifugation at $800 \times g$ for 10 min, resuspended in 5 ml of Superbroth (Burton et al., 1991) containing ampicillin (100 μg/ml), tetracycline (25 μg/ml) and kanamycin (50 μg/ml), and IPTG was then added at a final concentration of 250 μM. The culture was incubated overnight at 37 °C with vigorous agitation. The recombinant phages (supernatant) were collected by centrifugation for 10 min at $3000 \times g$ and filtered through a 0.45-μm filter. Phage-displayed HUC2-13 scFv mAbs from pCPDS and His-pCPDS were named HUC2p-1 and HUC2p-2, respectively. Soluble scFv antibodies, which were prepared using non-amber suppressor cells (SOLR strain; Stratagene), were obtained as bacterial culture supernatants. The soluble HUC2-13 scFv mAbs from pCPDS and His-pCPDS were referred as HUC2s-1 and HUC2s-2, respectively. Phage-displayed and soluble HUC2-13 scFv from pPDS (HUC2p and HUC2s, respectively) were used as controls.

2.6. Detection of chicken Cλ

In order to determine the expression of the chicken Cλ sequence, the recombinant phages (4.0×10^{10} CFU/ml) constructed by pCPDS, His-pCPDS and pPDS vector alone were subjected to sandwich ELISA. The plates (Maxisorp Nunc-Immuno™ module, Nunc, USA) were coated with 50 ng/well of anti-mouse κ antibody (Southern Biotechnology, USA) and anti-chicken light (λ) antibody (Bethyl Laboratories, USA), respectively, and blocked with 25% BlockAce (Yukijirushi, Japan) in PBS at 37 °C for 1 h. Phages were then added to each well (50 μl/well) and incubated at 37 °C for 1 h. Bound phages were detected using a peroxidase-labeled anti-M13 phage antibody (Amersham Biosciences, USA). After washing the plates, *o*-phenylene diamine sulfate was added and optical density was measured at 492 nm.

2.7. ELISA

ELISA plates were coated with 50 μl/well (2.5 μg/ml) of H25 peptide or BSA (control antigen) at 4 °C overnight. Plates were blocked with 350 μl/well of PBS containing 25% BlockAce at 37 °C for 2 h. The recombinant mAbs were then added to each well (50 μl/well) and the plates were incubated at 37 °C for 1 h. Bound mAbs were detected using a peroxidase-labeled anti-chicken λ chain antibody (Bethyl Laboratories). After washing the plates, *o*-phenylene diamine sulfate was added and the optical density was measured at 492 nm. The culture supernatant of the HUC2-13 hybridoma cells was used as a positive control.

2.8. Purification of the scFv antibody

Purification of HUC2s-1 and HUC2s-2 was first conducted using an anti-FLAG M2 affinity gel (Sigma) or nickel ion-charged Chelating Sepharose Fast Flow (Amersham Biosciences, Sweden) and then by using HiPrep Sephacryl S-200 HR (Amersham Biosciences, Sweden), according to manufacturers' instructions. The concentrations of purified HUC2s-1 and HUC2s-2 were determined with a Protein Assay kit (BIO-RAD, USA). For SDS-PAGE, purified mAbs (20 μg/lane) was electrophoresed in a 15% polyacrylamide gel and stained with CBB-R250. ELISA was performed as described above.

2.9. Western blotting

The equivalent of 50 μg of 10% mouse brain homogenate was separated using 13.5% polyacrylamide gels and then transferred to an Immun-Blot™ PVDF membrane (BIO-RAD, USA) at 200 mA for 2 h. Membranes were blocked with PBS containing 8% skim milk (Becton Dickinson, USA), 0.2% Tween 20 and 2.5 mM EDTA for 2 h at room temperature. Blots were developed by peroxidase-conjugated anti-chicken λ or anti-mouse κ antibodies (Southern Biotechnology) and anECL system (Amersham Biosciences, Sweden).

For expression analysis of FLAG in the recombinant scFv antibodies, the recombinant mAbs were assessed by Western blotting analysis using biotin-labeled anti-FLAG (Sigma) or peroxidase-labeled anti-mouse κ antibodies.

3. Results and discussion

3.1. Vector construction

Gene conversion is the main contributor to antibody diversification in chicken (Bernard et al., 1978; Sakano et al., 1980), in contrast to the mammalian mechanism, which involves gene rearrangement of functional V, J and D segments (Reynaud et al., 1985, 1987, 1989; Thompson and Neiman, 1987). It was reported that this gene conversion was not observed at the 3′ region of framework 4, derived from Jλ or JH, or the 5′ region of framework 1, derived from Vλ or VH, during the processes of diversification (McCormack and Thompson, 1990). This allows RT-PCR of the V region repertoire to be performed with only one pair of primers. Furthermore, it became evident that techniques for obtaining phage-displayed chicken antibodies is simpler than previously reported methods for obtaining phage-displayed mouse antibodies (Davies et al., 1995; Yamanaka et al., 1996; Jennifer et al., 2000).

Phage-displayed chicken mAbs were recently generated from immunized chicken spleen cells (Yamanaka et al., 1996) and chicken hybridoma cells (Nakamura et al., 2000) by using the mouse-antibody expression vector pPDS, which contains the mouse Cκ sequence as a tag (Yamanaka et al., 1995, 1996). However, cross-reactions between the recombinant chicken mAbs obtained from the vector and mouse immunoglobulins (Igs) may have adverse effects on the application of recombinant chicken mAbs. For example, background staining was observed due to cross-reaction with endogenous Igs in immunohistochemistry using mouse tissue, and due to artificial reactions by secondary antibodies directed towards mouse Igs in a sandwich ELISA system using recombinant chicken mAb and a mouse mAb.

To overcome these problems, we constructed the expression vectors pCPDS and His-pCPDS. The former vector was designed to express scFv, chicken Cλ and FLAG tags, fused with the carboxy-terminal half of coat protein III (cp3) at the 218th amino acid under the control of the lactose promoter based on the pPDS structure (Fig. 1A). The ribosome-binding site and the leader sequence of cp3 were followed by *Eag*I and *Bss*HII restriction sites for cloning. The stop codon, TAG, was inserted between the FLAG and cp3 sequences in order to generate soluble antibody fragments in non-suppressor strains of *E. coli*. (Marks et al., 1991; Hoogenboom et al., 1991) (Fig. 1B). Added to the latter vector was a 6 × histidine tag based on pCPDS to allow purification of the scFv mAb from the vector under neutral pH conditions (Fig. 1C). Both vectors were adjusted in terms of number of bases in an scFv-cloning site in order to allow a mock tag to be expressed.

3.2. Expression of chicken Cλ and FLAG

Chicken Cλ expression in the two vectors was determined by sandwich ELISA. Phages produced from pCPDS and His-pCPDS without the HUC2-13